On The Spatial Distribution of the Wave Energy Resource in Puerto Rico and the United States Virgin Islands

Miguel F. Canals-Silander[b], Carlos G. García Moreno[b]

[a] *UPRM Center for Applied Ocean Science and Engineering, Department of Engineering Science and Materials, University of Puerto Rico at Mayaguez, Mayaguez, Puerto Rico 00681-9000*
[b] *Coastal Observing Research and Development Center, Scripps Institution of Oceanography, University of California San Diego, La Jolla, CA 92037*

Abstract

The present article describes a numerical modeling study of the spatial distribution of the wave energy resource for Puerto Rico and the United States Virgin Islands (USVI). The study consists of an analysis of three years of output from the CARICOOS Nearshore Wave Model, an operational model based on the Simulating Waves Nearshore (SWAN) model. Using the wave model output, the wave power was computed and then averaged for a three year period from between January 1 2013 to December 31 2015. Maximum values at nearshore areas range from 7-8 kW/m for those locations in Puerto Rico exposed to North Atlantic winter swells, particularly the region between the towns of Aguadilla and Fajardo. This region is likely the most viable location for wave power generation in the US Caribbean given the very narrow shelf and the proximity to some of the most important components of Puerto Rico's electric grid. Wave power extraction certainly presents an interesting possibility for the future, and the present study is a first step towards better understanding the feasibility of such projects for the PR/USVI archipelago.

Keywords: Wave Energy, Wave Modeling, Waves in Puerto Rico / USVI, Renewable Energy, Wave Energy Converters

1. Introduction

The dependence of modern society on fossil fuel for power generation is slowly decreasing in order to increase power generation from clean renewable energy sources. From an availability perspective, one of the most promising renewable energy sources is the energy content of ocean waves. For the United States alone the naturally available wave energy resource at the continental shelf is estimated to be about 2,640 TWh/yr [1]. However, further research and development must take place before wave power can become a major player in the utility-scale power generation sector.

While the technology of wave energy conversion keeps improving and becoming more economical and reliable, detailed assessments of the availability of wave energy resources at candidate locations must be carried out in parallel.

*Corresponding author.
Email addresses: miguelf.canals@upr.edu (Miguel F. Canals-Silander), carlosgarcia@ucsd.edu (Carlos G. García Moreno)

Insular regions without significant oil or gas resources, such as Puerto Rico (PR) and the United States Virgin Islands (USVI), generally pay higher electricity prices than the US mainland. In addition, insular regions have a higher coastline length to surface area ratio, providing greater access to the ocean and, potentially, to marine renewable energy resources.

Other insular regions have made great strides in quantifying wave energy potential. For example, the wave energy resource for the Hawaiian archipelago has been analyzed in detail during the last decade, with several studies concluding that Hawaii has wave energy levels suitable for utility scale power generation [e.g. 2, 3]. Using preliminary estimates from coarse resolution wave models, [4] have identified wave energy as one of the most important renewable energy sources for Puerto Rico. However, there are no studies which adequately analyze the spatial distribution of the wave energy resource in the PR/USVI archipelago.

The ability to simulate the temporal and spatial distribution of sea state parameters is vital to explore the feasibility of wave energy extraction projects and to optimize the design of wave energy farms. The purpose of this paper is to provide a first look at the spatial structure of the annually averaged wave power density for the PR/USVI archipelago using three years of wave model data. The wave model used for wave energy estimation, as well as the validation process of such model, are described in section 2. Spatial maps of the annually averaged wave power distribution as well as its temporal variability are discussed in section 3, and concluding remarks are provided in section 4.

2. Methods

2.1. Numerical Model Description

The CARICOOS Nearshore Wave Model (CNWM) is an operational model based on the Simulating Waves Nearshore (SWAN) spectral wave model, which is described in detail in [5] and [6]. Details of the model setup and validation may be found in [7] and [8], and only the most important aspects of the model setup specific to this study are given here. The CNWM SWAN model is run in third generation mode, which includes model physics such as quadruplet interactions, expotential wind wave growth and whitecapping [6]. Model physics also include wave energy dissipation due to bottom friction using the JONSWAP formulation, triad wave interactions, diffraction and depth-induced wave breaking [6]. Figure 1 shows a schematic of the model grid and boundary conditions. The blue line represents the extent of the model grid at 1 km spatial resolution, and the red dots represent locations at which full two-dimensional spectral wave data from the NOAA NCEP Multigrid WaveWatch III Model [9] is provided as boundary conditions to the SWAN model. The operational model is run for 120 hours in forecast mode and nine hours in hindcast mode. Surface wind forcing is provided to the model from the National Weather Service National Digital Forecast Database, which consists of three days of wind forecasts from the WRF wind model, run operationally by the National Weather Service San Juan Office, and two days from the NOAA Global Forecast System (GFS, `http://www.emc.ncep.noaa.gov/GFS/.php`) atmospheric model. Grid bathymetry is obtained from the National Geophysical Data Center Digital Elevation Model for Puerto Rico and the United States Virgin Islands [10]. The

model runs operationally twice per day as soon as the NOAA WWIII spectral files for the 00Z and 12Z runs are available online, which usually occurs at around 06Z and 18Z, respectively.

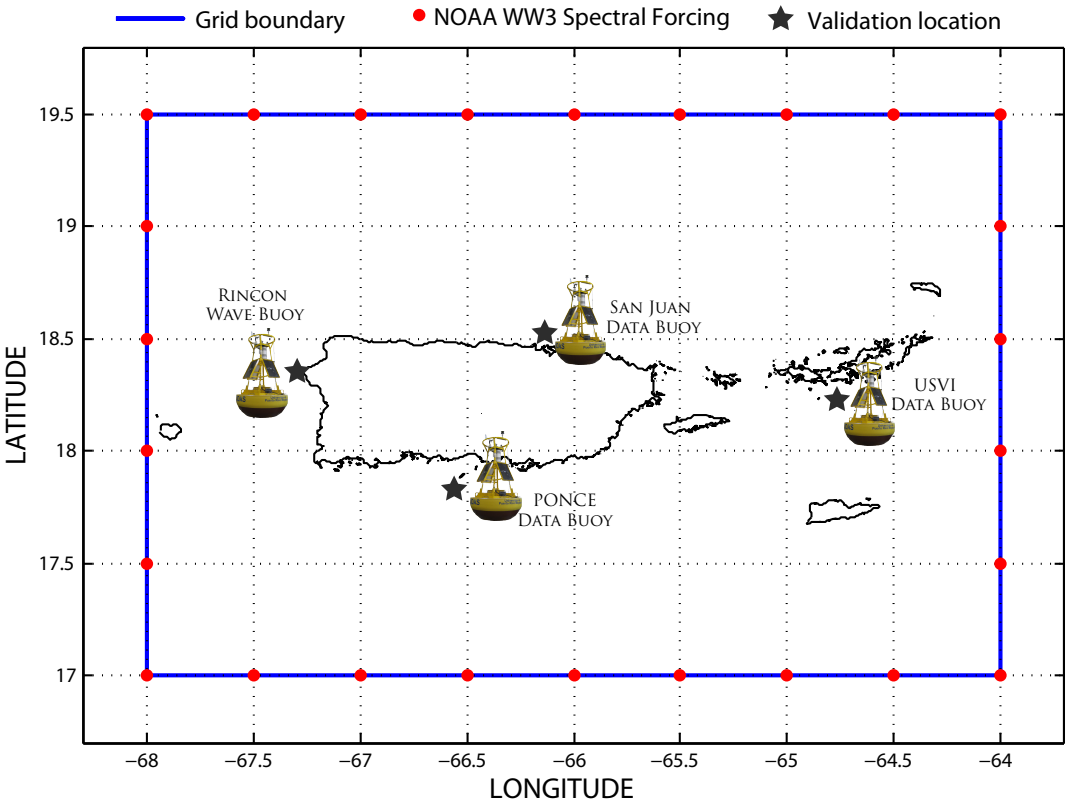

Figure 1: Schematic of the CARICOOS Nearshore Wave Model grid and boundary forcing. The blue line represents the extent of the model grid at 1 km spatial resolution, and the red dots represent locations at which full two-dimensional spectral wave data from the NOAA NCEP Multigrid WaveWatch III Model [9] is provided as boundary conditions to the SWAN model. The four buoy locations shown represent the sites at which the model was validated.

2.2. Model validation

In order to evaluate model performance, model output from October 29 2012 to January 31 2013 was compared with wave observations at four ocean data buoys owned and maintained by the Caribbean Coastal Ocean Observing System (CARICOOS, `http://www.caricoos.org`). The locations of these buoys are shown in Figure 1, and each buoy represents a distinct wave regime within the Puerto Rico / USVI region. The San Juan buoy, located about a kilometer off the city of San Juan in approximately 35 meters depth, is exposed to large North Atlantic swells and the persistent wind seas caused by easterly trade winds. The Rincón wave buoy is located about 1.5 kilometers off the coast in water about 33 meters deep and is relatively protected from easterly wind seas, but is fully exposed to long period winter swells entering the Mona Passage from the northwest, north and northeast. The USVI buoy is located about 14 kilometers south of St. John in about 60 meters depth and is significantly sheltered from winter swells by

St. Thomas and St. John to the north, but is fully exposed to wind seas from easterly trade winds as well as to long period swells that enter the Caribbean through the Anegada Passage. Finally, the Ponce buoy is located south of Puerto Rico at a depth of 17 meters, is sheltered from winter swells and is mostly affected by wind seas. All four buoys are periodically subject to strong wave events from tropical storms and hurricanes.

2.3. Estimating wave power density

In order to understand the spatial distribution of the annually averaged wave power density, three years of hourly model output was obtained from the CARICOOS Nearshore Wave Model. Since the CNWM runs operationally twice per day, the first 12 hours of each model run were extracted and combined in order to obtain the best available model output for a particular 24 hour period. The wave power density (in kW) per meter of wave crest is given by:

$$P = EC_g \tag{1}$$

where E is the wave energy density per unit area and C_g is the wave group speed. The wave energy density per unit area E for random waves is given by:

$$E = \frac{1}{16}\rho g H_s^2 \tag{2}$$

where H_s is the significant wave height, ρ the seawater density, and g the gravitational constant. The wave group speed, C_g, is given by:

$$C_g = \frac{1}{2}\left\{1 + \frac{4\pi d/L_e}{\sinh(4\pi d/L_e)}\right\}\frac{L_e}{T_e} \tag{3}$$

where d is the local water depth, T_e is the wave energy period [11], and L_e is the local wavelength of a wave with period T_e. The wave energy period is defined as

$$T_e = T_{-10} = \frac{m_{-1}}{m_0} \tag{4}$$

where m_n is the n-th moment of the two-dimensional wave spectrum $S(f,\theta)$, given by

$$m_n = \int_0^{2\pi}\int_0^{\infty} f^n S(f,\theta) df d\theta \tag{5}$$

where f and θ represent frequency and wave direction, respectively. The reader is referred to Appendix A in [1] for a detailed discussion of equations 1 through 5. Unfortunately, in many cases T_e is not a common variable reported by oceanographic buoys or numerical wave models. Without knowing the full spectral shape of the sea state at a specific location it is not possible to determine the exact value of T_e, and this value must be approximated using either the mean wave period T_m or the peak wave period T_p, or a combination of these values. In our case, full spectral output is provided by SWAN but only at discrete locations throghout the domain. However, SWAN provides spatial output

of commonly used wave parameters such as significant wave height, peak period, mean period, among other integral parameters. When there are no accurate estimates of T_e, estimates of T_e based on the peak period or the mean period have been used to estimate available wave power. A commonly used but rather crude estimate is $T_e = 0.9T_p$, which is equivalent to assuming a JONSWAP spectral shape with a value of $\gamma = 3.3$ for the peak enhancement factor [11]. This type of estimate was used, for example, by [12] to estimate available wave energy in the East China Sea.

In the present study the SWAN wave model does provide full spectral output but only at discrete locations. In order to estimate T_e for the full domain, we have developed a multivariate polynomial regression using MATLAB to estimate T_e based on T_p and T_m so that T_e can be estimated throughout the full spatial extent of the SWAN model grid. Using three years of full 2D spectral output at three locations on the north coast of Puerto Rico and the US Virgin Islands, a 2D multivariate polynomial was determined to be the best estimator of T_e:

$$T_e = c_1 T_m^2 + c_2 T_m T_p + c_3 T_m + c_4 T_p^2 + c_5 T_p + c_6 \tag{6}$$

where the parameters are $c_1 = -0.0129, c_2 = 0.0641, c_3 = 0.2181, c_4 = -0.0107, c_5 = 0.1030, c_6 = 2.8350$. Figure 2 shows a comparison between the energy period (T_e) values derived from SWAN model spectra (thick blue line, computed using equation 4) and the estimated T_e values using 2D multivariate regression (red line, equation 6) for three locations in the model domain at the 30m depth contour: Arecibo, San Juan and north of St. Thomas. These are the same locations used in section 3.4 to estimate the cumulative wave power. The scatter plot for each location includes the correlation coefficients and the root mean square error. From this figure it is evident that equation 6 provides a very good estimate of the energy period T_e based on a 2D polynomial fit which is a function of the model-computed T_p and T_m values.

Using the estimates for T_e, the local wavelength L_e is then obtained by solving the full wave dispersion relation:

$$\omega^2 = gk \tanh kd \tag{7}$$

where $\omega = 2\pi/T_e$ is the wave angular frequency and $k = 2\pi/L_e$ is the wavenumber. For this study the wavelength as a function of time and space has been obtained by solving the above dispersion relation equation using the Newton-Raphson method. The wave power per unit meter of wave crest, P, has been computed at each grid point for the three year period between January 1 2013 to December 31 2015. Model validation results will be presented in the following section.

3. Results and Discussion

3.1. Model validation

Figure 3 shows a comparison between the observed and simulated significant wave height and peak period at the four CARICOOS buoys: Rincón (top row), San Juan (second row from top), Ponce (third row from top) and USVI

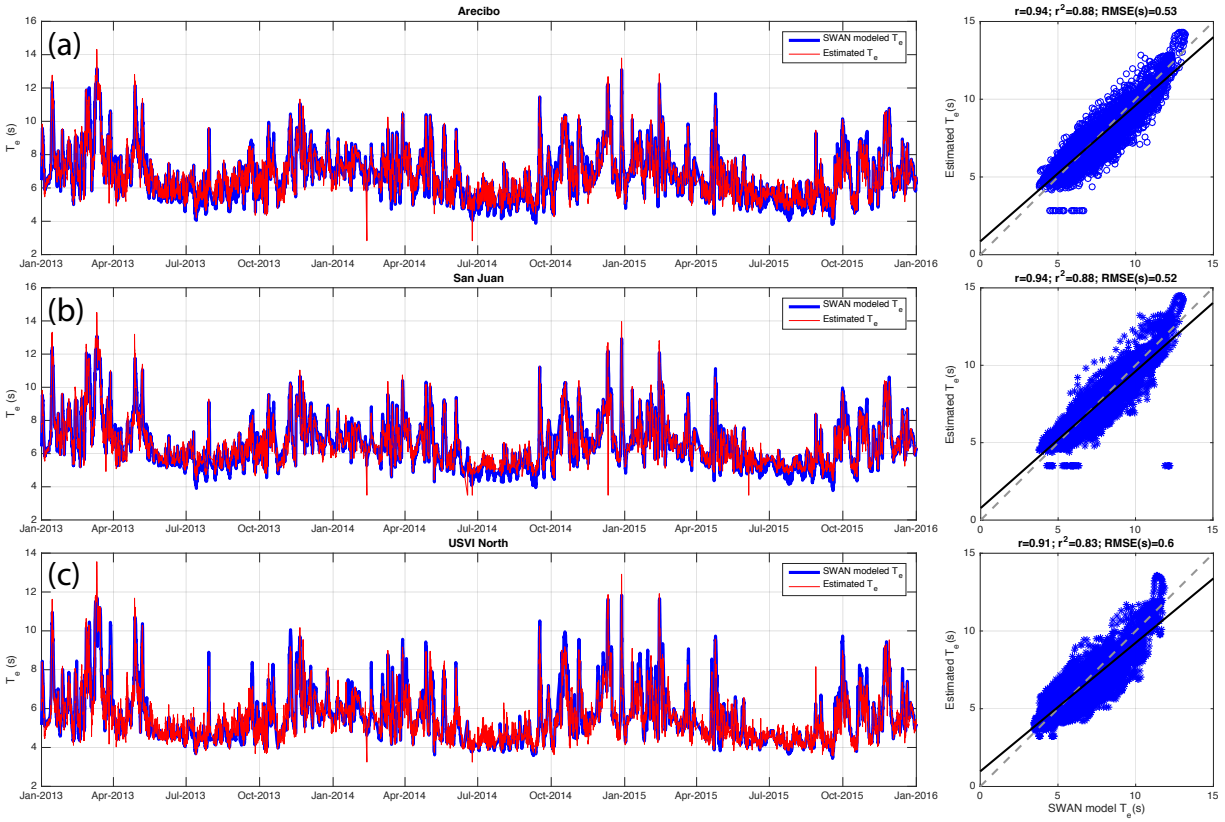

Figure 2: Comparison between the energy period (T_e) values derived from SWAN model spectra (thick blue line) and the estimated T_e values (red line) using 2D multivariate regression (equation 6) for three sites at the 30 meter depth contour: Arecibo (top panels), San Juan (middle panels), and north of St. Thomas (bottom panel). The scatter plot for each location includes the correlation coefficients and the root mean square error.

(bottom row). Visual inspection suggests that the model reproduces correctly the wave heights and peak periods of significant wave events, although the model underestimates the wave height for several major events, especially in the San Juan and Rincón buoys. This discrepancy could be due to an underestimation caused by Wavewatch III boundary conditions, or due to small scale wind effects not accurately predicted by the wind model used to force SWAN. No validation statistics for wave direction are included here for brevity, but wave direction has previously been validated in our model [7].

Figure 4 shows scatter plots of observed vs. simulated significant wave height (left column) and observed vs. simulated peak wave periods (right column) at the four CARICOOS buoys. For the significant wave height scatter plots the color of each data point represents the observed peak period at that instance. The color of each data point in the peak wave period scatter plots (right column) represents the observed significant wave height at that instance. This visualization shows how the model behaves as a function of the observed sea state. The solid black line in each plot represents the linear regression which best represents the model-data relationship, while the gray dashed line represents a perfect fit. In general, the model underestimates wave heights at all four buoys, with a more pronounced

underestimation at Rincón. The predictions of peak wave periods are generally worse for low wave periods. This could be due to the challenges associated with predicting the coastal wind field, including the daily sea breeze cycle. Another possibility is that during low wave conditions the wind seas and swell can have similar energy levels, making it difficult for both the buoy and the model to identify the correct spectral energy peak corresponding to the peak wave period.

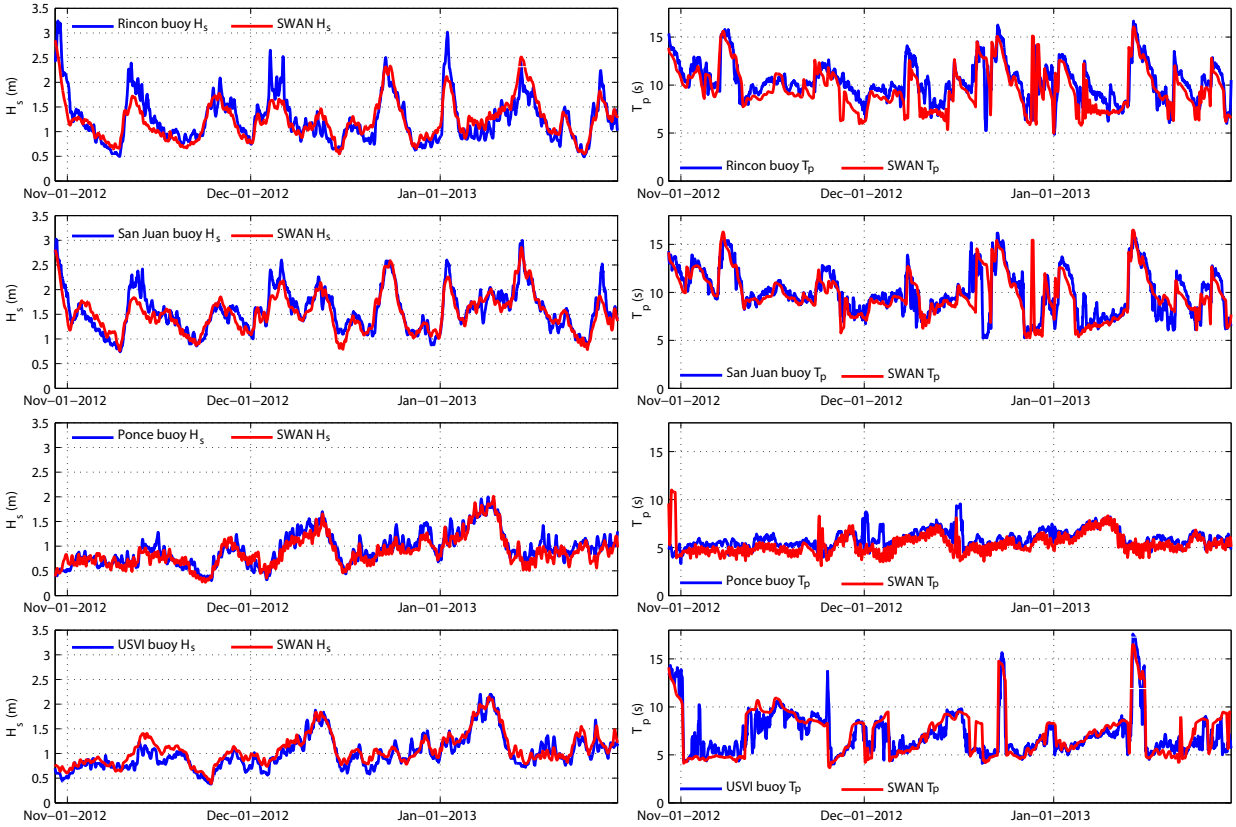

Figure 3: Comparison between observed (blue line) and simulated (red line) significant wave height (left column) and peak period (right column) at the four CARICOOS buoys: Rincón (top row), San Juan (second row from top), Ponce (third row from top) and USVI (bottom row).

Table 1 shows the model validation statistics, including the least squares fit, for both significant wave height and peak wave period for each buoy location. As suggested by the plots shown in Figure 4, the model does a much better job at predicting the significant wave height than in predicting peak wave periods, especially in Ponce which is dominated by wind seas. In general, however, it can be concluded that the model does a good job of capturing the temporal and spatial variability of the wave field around Puerto Rico and the US Virgin Islands, especially at the most energetic locations exposed to North Atlantic swells.

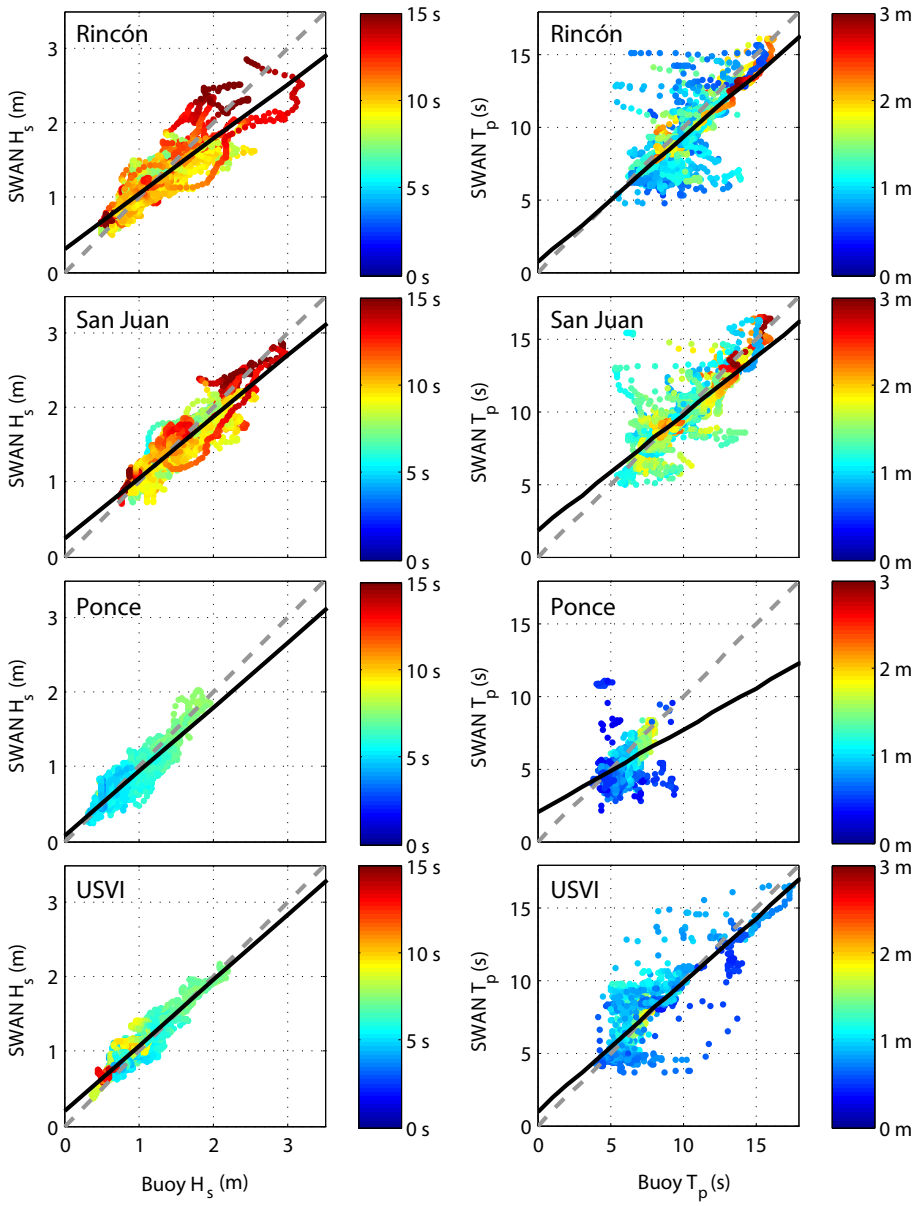

Figure 4: Left column: Scatter plots of observed vs. simulated significant wave height at the four CARICOOS buoys: Rincón (top), San Juan (second from top), Ponce (third from top) and USVI (bottom); the color of each data point represents the observed peak period at that instance. Right column: Same as the left column but for the peak wave period; the color of each data point represents the observed significant wave height at that instance. The solid black line in each plot represents the linear regression which best represents the model-data relationship, while the gray dashed line represents a perfect fit.

3.2. Annual average wave power density

The yearly averaged wave power for calendar years 2013, 2014 and 2015 is shown in Figure 5. While it is difficult to draw conclusions from just three years of data, it is evident that there is significant annual variability in the available wave power density.

	H_s				T_p			
	r	r^2	RMSE (m)	Least Squares Fit	r	r^2	RMSE (s)	Least Squares Fit
Rincón	0.86	0.75	0.24	$H_{s_{SWAN}} = 0.73H_{s_{buoy}} + 0.33$	0.76	0.58	1.64	$T_{p_{SWAN}} = 0.83T_{p_{buoy}} + 0.98$
San Juan	0.90	0.815	0.19	$H_{s_{SWAN}} = 0.81H_{s_{buoy}} + 0.25$	0.80	0.63	1.48	$T_{p_{SWAN}} = 0.77T_{p_{buoy}} + 2.05$
Ponce	0.91	0.835	0.15	$H_{s_{SWAN}} = 0.85H_{s_{buoy}} + 0.08$	0.46	0.21	1.14	$T_{p_{SWAN}} = 0.55T_{p_{buoy}} + 2.16$
USVI	0.93	0.865	0.14	$H_{s_{SWAN}} = 0.88H_{s_{buoy}} + 0.20$	0.83	0.69	1.39	$T_{p_{SWAN}} = 0.89T_{p_{buoy}} + 0.97$

Table 1: Model validation statistics at each buoy location.

Figure 6 shows the spatial structure of the annually averaged wave power density field for the period between January 1 2013 to December 31 2015. The black dashed line represents the 30-m depth contour. The red stars indicate the three locations at the 30-m depth contour at which the percent occurrence matrix for H_s and T_e have been analyzed (see next subsections). Average values for areas close to the northern coasts of Puerto Rico range from 7-8 kW/m for the modeled period. Note the much larger power densities in Anegada Island to the top right of the figure. Coastal areas in northern USVI show much smaller power densities. For west, east and south-facing areas of Puerto Rico and the USVI average values are very small, on the range of 2-3 kW/m. There is a zonally homogeneous distribution of average wave power between Fajardo (easternmost part of Puerto Rico) and Aguadilla (westernmost corner with north-facing coastlines) with values close to the coast between 7-8 kW/m. This region is likely the most viable location for wave power generation in the US Caribbean given the very narrow shelf and the proximity to some of the most important components of Puerto Rico's electric grid.

Wave power in the USVI is much lower than that found off the northern coast of PR. For the case of St. Thomas and St. John, the shallow depths of the USVI shelf lead to significant wave refraction and dissipation due to friction, leading to a significant reduction in the energy of the incoming wave field. For St. Croix, maximum power density levels of 5-6 kW/m are only present at the eastern-most end of the island and are much less for the rest of its coastline. Particularly interesting is a shadow zone in wave power density north of St. John caused by wave refraction and dissipation due to the shallow depths of the USVI shelf. This leads to smaller wave power densities than would have been expected given that these islands would appear to be fully exposed to winter swells coming from the north.

3.3. Seasonal variability

Figure 7 shows the monthly-averaged wave power density for each month for the modeled period. Results show a well-defined annual cycle in wave power with strong seasonal variability, with largest wave power densities ocurring near north-facing areas and during the months between November and March. During these months, long-period winter swells caused by cold fronts and North Atlantic winter storms dominate the wave climate. Swell events typically last several days with peak significant wave heights ranging from 2-6 meters and peak periods from 10-20 seconds. The dominant direction for these events is from the northwest, north or northeast. While it is difficult to

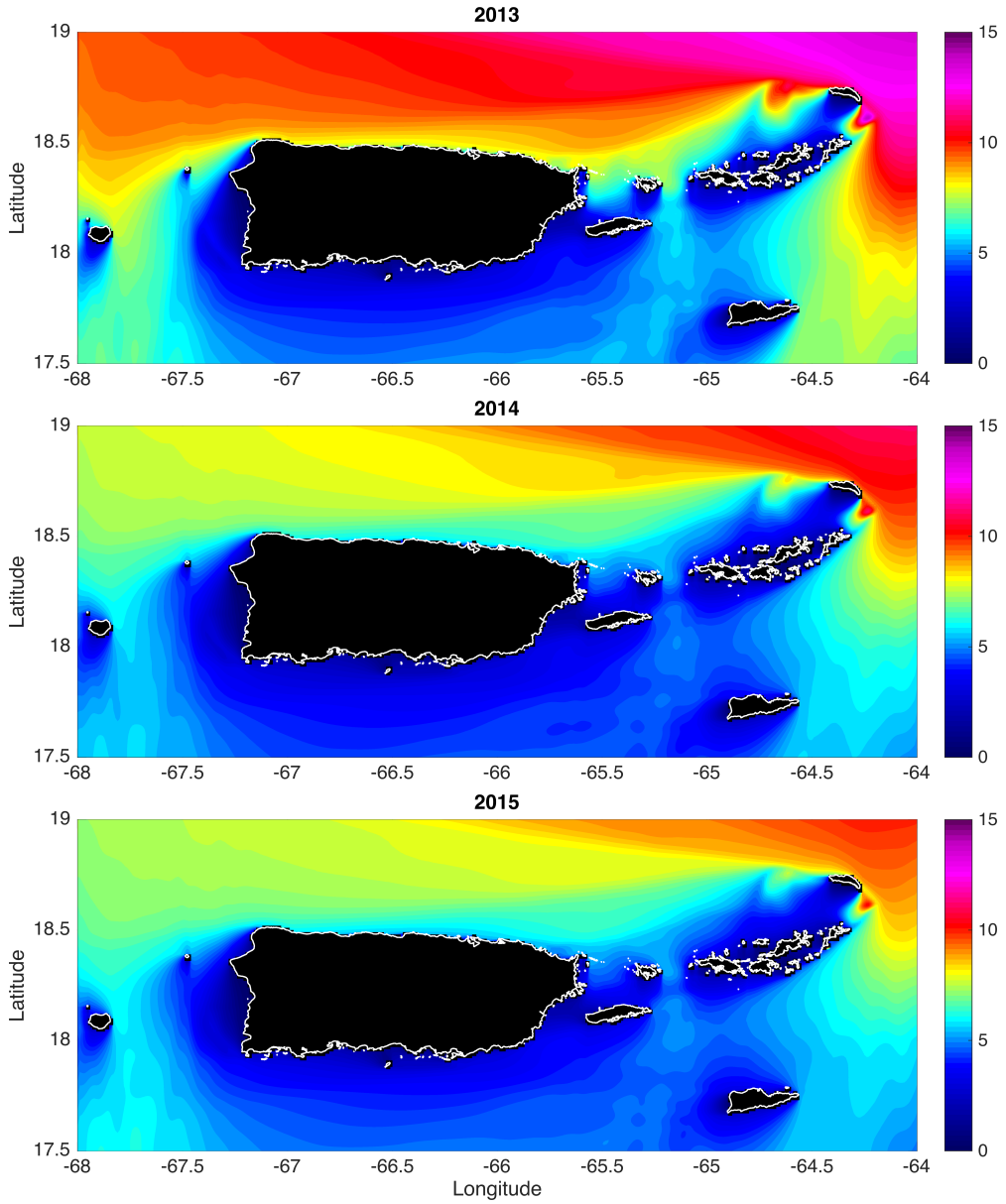

Figure 5: Average wave power density (kW/meter) for calendar years 2013 (top panel), 2014 (middle panel) and 2015 (bottom panel).

capture interannual variability with only three years of model output, it is well known that winter swells in the North Atlantic, including those affecting the Caribbean, are strongly modulated by the North Atlantic Oscillation [13].

3.4. Cumulative wave power

To better understand the structure of the wave climate at locations with relatively high wave energy potential, three coastal sites located on the 30-m depth contour were selected: two on the north coast of Puerto Rico (Arecibo and San Juan) and one site north of St. Thomas, as shown on Figure 6. Figure 8 shows the percent occurrence matrix of

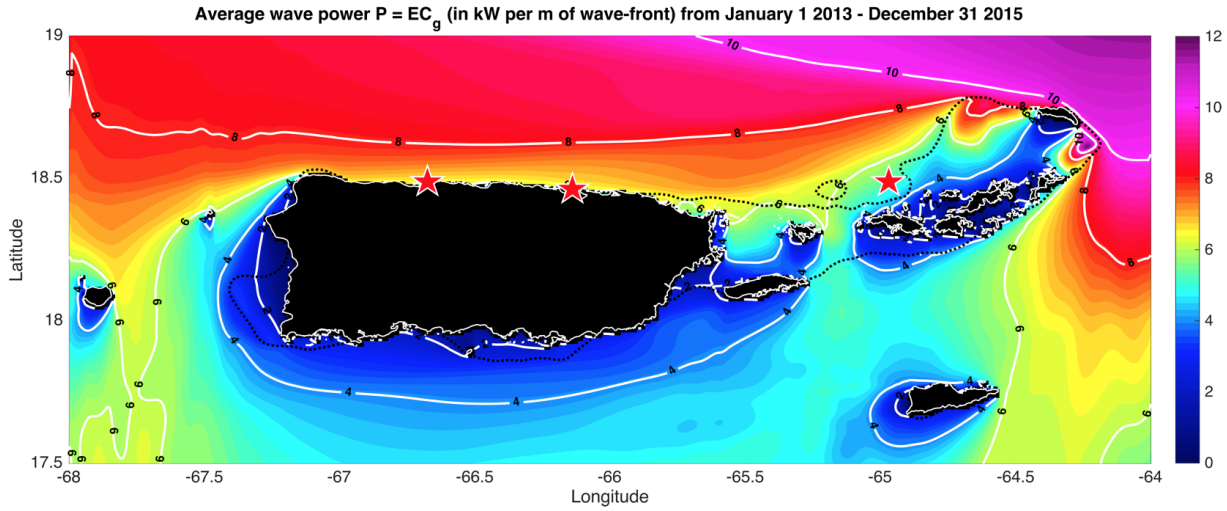

Figure 6: Top: Average wave power density (kW/meter) from January 1 2013 to December 31 2015. The red stars indicate the three locations at which the percent occurrence matrix for H_s and T_e was computed.

H_s and T_e for each of these sites for the simulation period. White contours represent the wave power for each $H_s - T_e$ pair. The colored contours represent the wave energy per meter of wave crest (MWh/m) as a function of each $H_s - T_e$ pair.

Several regions that contribute a significant fraction of the available energy level at each site can be observed from Figure 8. Sea states with wind seas with H_s between 1 and 2 meters and with T_e between 4 and 6 seconds are dominated by persistent trade winds at all three sites. Another region corresponding to a large percentage of the available wave energy corresponds to sea states with T_e between 6 and 9 seconds. These sea states are dominated by moderate winter swells and are much more energetic at the Arecibo and San Juan locations, as previously discussed. Large, long period wave events with T_e larger than 10-11 seconds, although very energetic, are somewhat rare and do not contribute much to the annually integrated wave energy level. All three sites have an annually averaged wave power density between 6-8 kW/m, with Arecibo and San Juan being the most energetic of the three at around 7.6 kW/m. For San Juan and Arecibo this translates into an average annual energy yields of 54 MWh/yr per meter of wave crest.

3.5. Implications for wave energy exploitation

The wave energy yields for three north-facing sites discussed above are comparable to values obtained by previous studies for the East Coast of the United States [1] and Mediterranean Sea [14], yet much smaller than other locations in the United States such as Oregon [15] and Hawaii [3]. From a global perspective, power densities ranging from 5 to 10 kW/m are considered to have a low wave energy resource. Despite being directly afected by winter swells and having a consistent easterly trade wind sea regime, wave energy resources in Puerto Rico and the US Virgin Islands fall into the low wave energy category when looking at the annually averaged power densities and available energy. However,

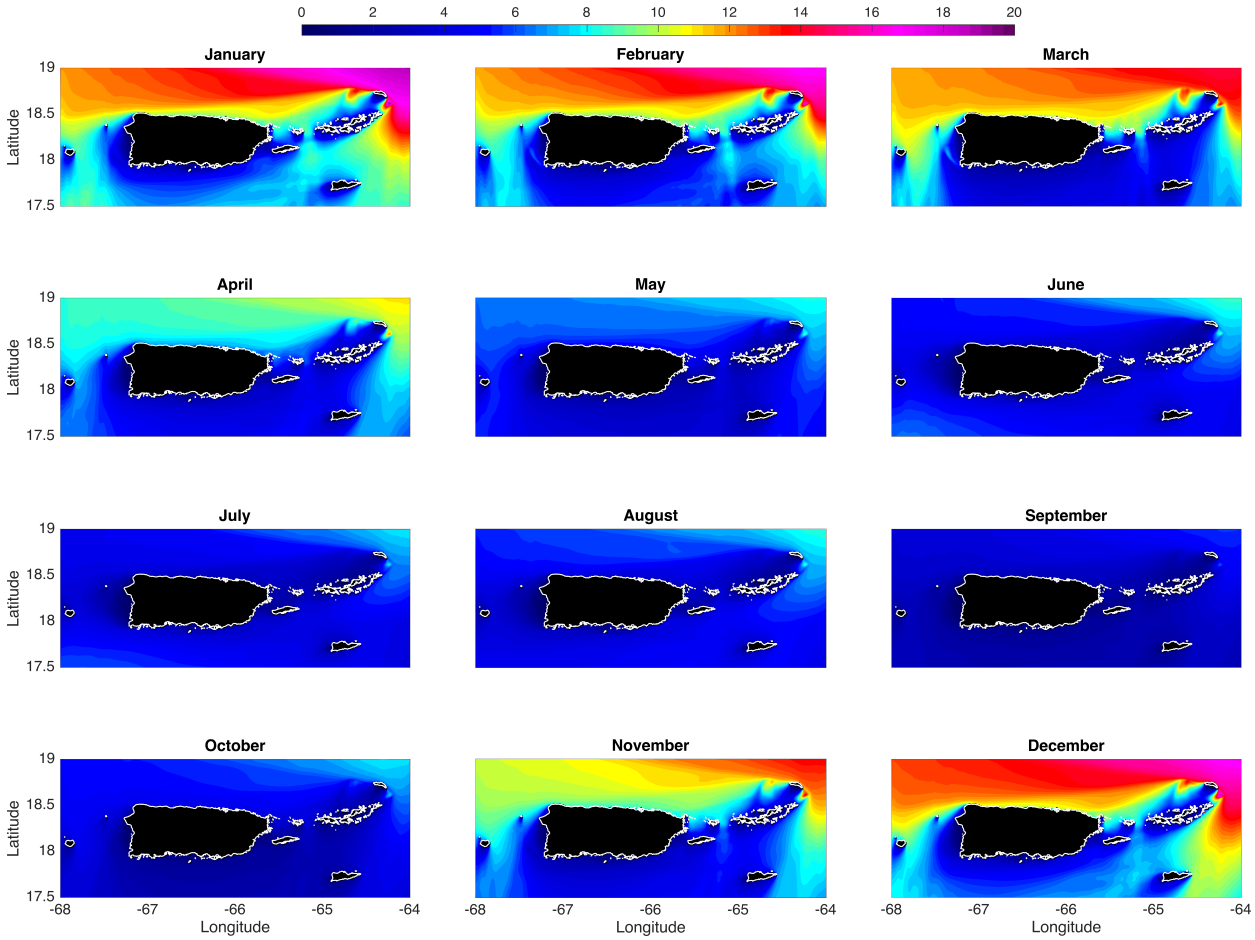

Figure 7: Average wave power in kW/m for each month, using model output from January 1 2013 to December 31 2015

the efficiency of wave energy converters and their potential for utility-scale power generation not only depend on the annual power level but on the spectral characteristics of the local wave climate. A wave energy converter (WEC) can be chosen and optimized to perform best according to the prevailing sea states, and the anually averaged power is not the only quantity to take into account when considering the feasibility of extracting power from waves. A WEC optimized for significant wave heights between 1 and 3 meters with energy periods between 4 and 10 seconds (or peak wave periods between 6 and 14 seconds) could very well be a feasible alternative for power generation in the region. Large, long period wave events with T_e larger than 10-11 seconds, although very energetic, are somewhat rare and do not contribue much to the annually integrated wave energy level.

For Arecibo and San Juan, two north-facing sites off the north coast of Puerto Rico, the average annual energy yield of 54 MWh/yr per meter of wave crest can be better put into context by comparing the amount of available wave energy to local demand for energy as published by the Puerto Rico Electric Power Authority (PREPA). In 2012 the industrial sector consumed 2,778,512 MWh, which accounts for almost 20% of the island-wide energy consumption. Using the average annual yield of 54 MWh/yr per meter of wave crest, this is the available wave energy in 60 km

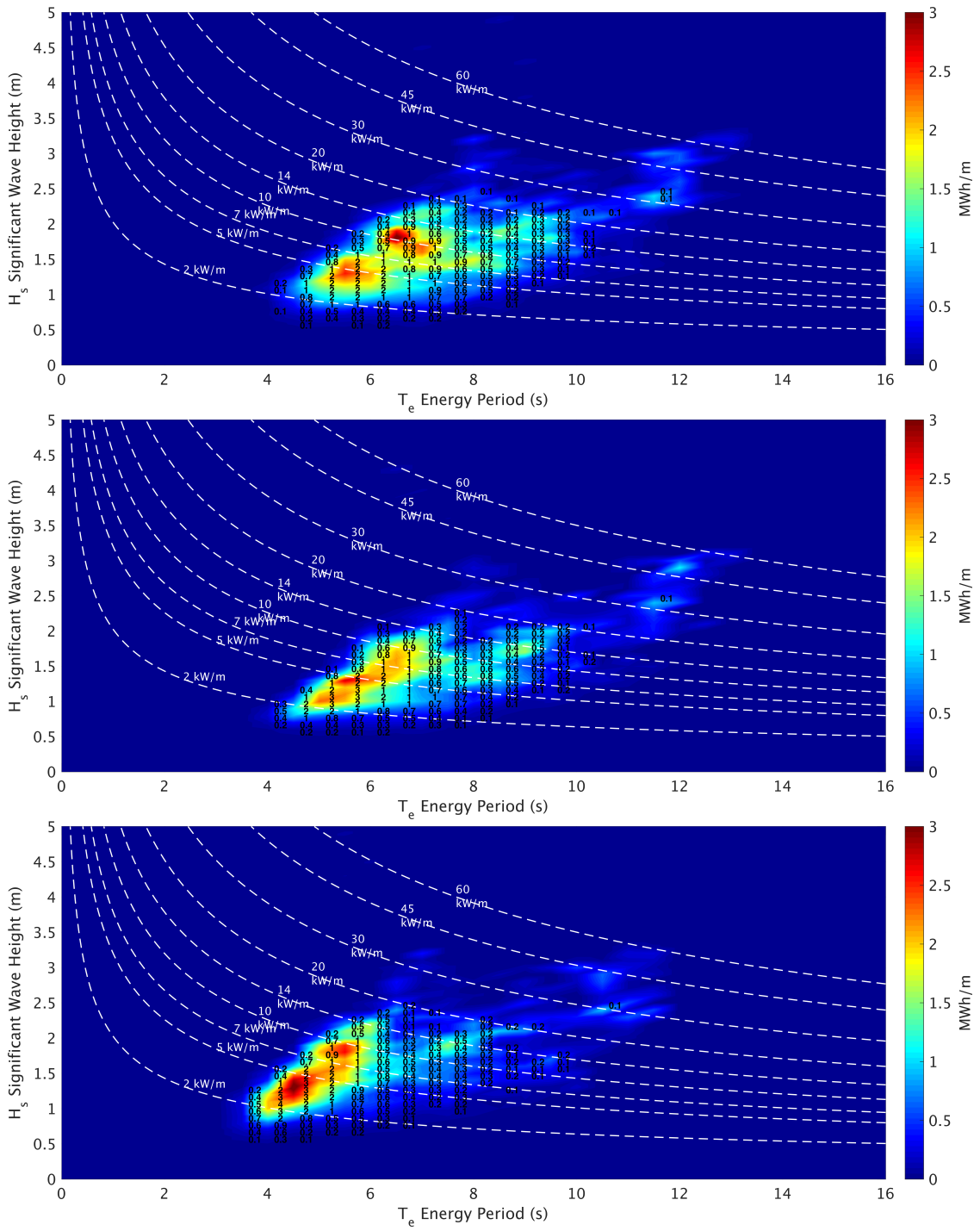

Figure 8: Three-year wave energy characterization for the three locations: Arecibo (top), San Juan (middle) and north of St. Thomas (bottom). Contour lines show instantaneous power density per meter of wave crest(kW/m) for a given pair of H_s and T_e. $H_s - T_e$ pairs are presented as percent of total occurrences on a scatter table (black text). The colormap depicts the wave energy per meter of wave crest (MWh/m) as a function of each $H_s - T_e$ pair.

of coastline off northern Puerto Rico. Even though this crude comparison does not take into acount WEC efficiency, or realistic WEC spacing and harvest area, it serves to show that at least a fraction of the energy consumed by the industrial sector could be satisfied with wave power.

4. Concluding Remarks

The spatial distribution of the annual average wave power throughout Puerto Rico and the United States Virgin Islands from 2013 to 2015 has been analyzed through the use of a high resolution spectral wave model. This wave model was validated using buoy data at four locations with different wave characteristics. In general, the model slightly underestimates the significant wave height and the peak wave periods, however, the model was able to correctly reproduce the most important features of the wave climate in the region and its performance was found to be satisfactory. Using the wave model output, the wave power was computed and then averaged for a three year period from January 1 2013 to December 31 2015. Maximum values at nearshore areas range from 7-8 kW/m for those locations in Puerto Rico exposed to North Atlantic winter swells, particularly the region between the towns of Aguadilla and Fajardo. This region is likely the most viable location for wave power generation in the US Caribbean given the very narrow shelf and the proximity to some of the most important components of Puerto Rico's electric grid. Monthly wave power averages were also computed and showed a clear seasonal pattern, with the highest wave power densities ocurring between November and March of each year. Interannual variability was not explored in detail since only three years of high-resolution wave model output were available, but future studies should examine the effects of low frequency variability (e.g. ENSO, NAO) on the wave power resource availability in the US Caribbean.

Given their insular nature and their almost complete dependence on fossil fuels for power generation, Puerto Rico and the USVI should look to the ocean as a way to diversify their power generation portfolio. Wave power extraction certainly presents an interesting possibility for the future, and the present study is a first step towards better understanding the feasibility of such projects for the PR/USVI archipelago.

Acknowledgements

The development of the CARICOOS Nearshore Wave Model was made possible thanks to the financial support from the NOAA-IOOS program (Grant Number NA11NOS0120035) and the University of Puerto Rico Sea Grant Program (Grant Number R-124-1-12). Carlos Anselmi from the National Weather Service San Juan Weather Forecast Office was the lead developer of the first version of the CARICOOS Nearshore Wave Model. The authors thank two anonymous reviewers who provided great feedback that improved the paper substantially.

References

References

[1] EPRI, Mapping and assessment of the United States ocean wave energy resource, Prepared for the U.S. Department of Energy, Electric Power Research Institute (2011).

[2] J. Stopa, K. Cheung, Y. L. Chen, Assessment of wave energy resources in Hawaii, Journal of Renewable Energy 36 (1) (2011) 554–567.

[3] J. E. Stopa, J.-F. Filipot, N. Li, K. F. Cheung, Y.-L. Chen, L. Vega, Wave energy resources along the hawaiian island chain, Renewable Energy 55 (2013) 305 – 321. doi:http://dx.doi.org/10.1016/j.renene.2012.12.030.
URL http://www.sciencedirect.com/science/article/pii/S0960148112007963

[4] A. Irizarry, J. Colucci, E. O'Neill, Achievable renewable energy targets for Puerto Rico's renewable energy portfolio standard, Prepared for the Puerto Rico Energy Affairs Administration, University of Puerto Rico at Mayaguez (2008).

[5] N. Booij, R. C. Ris, L. Holthuijsen, A third generation wave model for coastal regions. Part 1: Model description and validation, Journal of Geophysical Research C4 (104) (1999) 7649-7666.

[6] The SWAN Team, SWAN user manual, Technical report, Delft University of Technology (2012).

[7] C. Anselmi, M. Canals, J. Morell, J. Gonzalez, J. Capella, A. Mercado, Development of an operational nearshore wave forecast system for Puerto Rico and the U.S. Virgin Islands, Journal of Coastal Research 28 (5) (2012) 1049–1056.

[8] M. Canals, J. Morell, J. Corredor, S. Leonardi, Expanding the Caribbean Coastal Ocean Observing System into the nearshore region, in: Oceans, 2012, 2012, pp. 1–4. doi:10.1109/OCEANS.2012.6404936.

[9] A. Chawla, H. L. Tolman, V. Gerald, D. Spindler, T. Spindler, J.-H. G. M. Alves, D. Cao, J. L. Hanson, E.-M. Devaliere, A multigrid wave forecasting model: A new paradigm in operational wave forecasting, Weather and Forecasting 28 (2013) 1057–1078.

[10] L. A. Taylor, B. W. Eakins, R. R. Warnken, K. S. Carignan, G. F. Sharman, P. W. Sloss, Digital elevation models for San Juan and Mayagüez, Puerto Rico: Procedures, data sources and analysis, Technical report, NOAA National Geophysical Data Center, Boulder, CO (2006).

[11] A. M. Cornett, A global wave energy resource assessment, in: Proceedings of the 18th ISOPE conference, 2008.

[12] S. Wu, C. Liu, X. Chen, Offshore wave energy resource assessment in the east china sea, Renewable Energy 76 (2015) 628 – 636. doi:http://dx.doi.org/10.1016/j.renene.2014.11.054.
URL http://www.sciencedirect.com/science/article/pii/S0960148114007848

[13] D. K. Woolf, P. G. Challenor, P. D. Cotton, Variability and predictability of the North Atlantic wave climate, Journal of Geophysical Research: Oceans 107 (C10) (2002) 9–1–9–14, 3145. doi:10.1029/2001JC001124.
URL http://dx.doi.org/10.1029/2001JC001124

[14] D. Vicinanza, P. Contestabile, V. Ferrante, Wave energy potential in the north-west of sardinia (italy), Renewable Energy 50 (2013) 506 – 521. doi:http://dx.doi.org/10.1016/j.renene.2012.07.015.
URL http://www.sciencedirect.com/science/article/pii/S0960148112004417

[15] P. Lenee-Bluhm, R. Paasch, H. T. Özkan Haller, Characterizing the wave energy resource of the {US} pacific northwest, Renewable Energy 36 (8) (2011) 2106 – 2119. doi:http://dx.doi.org/10.1016/j.renene.2011.01.016.
URL http://www.sciencedirect.com/science/article/pii/S0960148111000383